Jurnal Teknologi Perikanan dan Kelautan
Vol. 17 No. 2, May 2026: 325-337

ISSN: 2087-4871
EISSN: 2549-3841
DOI: https://doi.org/10.24319/jtpk.17.325-337

OPEN ACCESS Check for updates

EVALUATION OF SEAWORTHINESS OF THE TRADITIONAL LONGBOAT IN TECHNICAL ASPECTS BASED ON MODELING AND SIMULATION

EVALUASI KELAIK LAUTAN PERAHU TRADISIONAL LONGBOAT DALAM ASPEK TEKNIS BERDASARKAN PEMODELAN DAN SIMULASI

Andie Murtono[1], Ahmad Ilham Ramadhani[2*], Heru Santoso[3], Ahmad Tubagus Tsani Risqi Aji[4], Muhammad Zainul Arifin[3], Louis Andre Ginto[5]

[1]Department of Fisheries Mechanization, Politeknik Kelautan dan Perikanan Bitung, Jl. Tandurusa, Aertembaga Dua, Aertembaga, Kota Bitung, North Sulawesi 95526, Indonesia
[2]Department of Mechanical Engineering, Universitas Muhammadiyah Surakarta, Jl. Ahmad Yani, Pabelan, Kartasura, Sukoharjo, Central Java 57169, Indonesia
[3]Department of Fishing Technology, Politeknik Kelautan dan Perikanan Bitung, Jl. Tandurusa, Aertembaga Dua, Aertembaga, Kota Bitung, North Sulawesi 95526, Indonesia
[4]Badan Pelatihan dan Penyuluhan Perikanan Tegal, Jl. Irian No.31, Panggung, Tegal Timur, Kota Tegal, Central Java 52122, Indonesia
[5]CV. Gudang Biru Bitung, Jl. Tandurusa, Aertembaga Dua, Aertembaga, Kota Bitung, North Sulawesi 95526, Indonesia
*Corresponding author: air436@ums.ac.id

(Received November 14, 2025; Revised June 14, 2026; Accepted June 29, 2026)

ABSTRACT

Traditional longboat fishing vessels have changed in model and shape due to fishing techniques. This research aims to evaluate the technical seaworthiness of longboats in planning fishing operations based on the results of vessel models according to the original shape. The technical evaluation includes observation, modeling, and simulation of operations at speeds of 4, 8, 12, and 16 knots on Maxsurf, and calculation of load and fuel. The results of the technical evaluation of the observations show that the longboat has been modified using Fiber-Reinforced Plastic (FRP) techniques. The vessel features a pointed bow, a flat stern, a sharp V-shaped bottom, and no outriggers. The results of the main dimension modeling were LoA 10.25 m, LwL 8.97 m; width 1.29 m; height 0.68 m; and draft 0.2 m, corresponding to the main measurement range from the observation results. The hydrostatic displacement value is 1.34 tons, the draft and immersion are 0.2 m, and the waterline height is along LwL. The operational simulations showed the estimated resistance and engine power (362.4 N; 1.25 HP), (1449.79 N; 10.02 HP), (2899.24 N; 30.02 HP), and (3528.56 N; 48.68 HP) at speeds of 4, 8, 12, and 16 knots, respectively. The total operational load was 1.29 tons, remaining below the displacement limit. Fuel consumption rates were estimated at 0.51, 4.14, 12.12, and 19.58 liters/hour at 4, 8, 12, and 16 knots, respectively. The technical aspects that have been obtained can be used as a reference for seaworthy planning in fishing operations.

Keywords: hydrostatic, longboat body, Maxsurf, resistance, voyage plan

ABSTRAK

Perahu nelayan tradisional jenis *longboat* telah berubah model dan bentuk dikarenakan aspek teknik penangkapan ikan. Penelitian ini bertujuan untuk evaluasi teknis kelaik lautan kapal *longboat* dalam perencanaan operasi penangkapan ikan berdasarkan hasil pemodelan kapal sesuai dengan bentuk asli. Evaluasi teknis meliputi: observasi, membuat dan simulasi operasi pada kecepatan 4, 8, 12, dan 16 knot pada Maxsurf, dan perhitungan muatan serta bahan bakar. Hasil evaluasi teknis pengamatan menunjukkan bahwa perahu *longboat* telah dimodifikasi menggunakan teknik *Fiber Reinforced Plastic* (FRP). Perahu tersebut memiliki haluan yang runcing, buritan yang datar, dasar berbentuk V yang tajam, dan tanpa cadik. Hasil pemodelan dimensi utama LoA 10,25 m; LwL 8,97 m; lebar 1,29 m; tinggi 0,68 m; dan draft 0,2 m, sesuai dengan rentang pengukuran utama dari hasil observasi. Nilai hidrostatis meliputi *displacement* 1,34 ton, *draft and immersed* 0,2 m, dan tinggi garis air berada sepanjang LwL. Simulasi operasi menunjukkan hambatan dan daya mesin (362,4 N dan 1,25 HP), (1449,79 N dan 10,02 HP), (2899,24 N dan 30,02 HP), dan (3528,56 N dan 48,68 HP) pada kecepatan 4, 8, 12, dan 16 knot, berturut-turut. Beban operasional total adalah 1,29 ton, tetap di bawah *displacement limit*. Tingkat konsumsi bahan bakar sebesar 0,51, 4,14, 12,12, dan 19,58 liter/jam pada kecepatan 4, 8, 12, dan 16 knot, berturut-turut. Aspek teknis yang telah diperoleh dapat dijadikan sebagai acuan perencanaan kelaik lautan kapal *longboat* dalam operasi penangkapan ikan agar operasi penangkapan ikan efektif, efisien, dan aman.

Kata kunci: hambatan, hidrostatis, *longboat body*, Maxsurf, rencana layar

INTRODUCTION

One type of fish variety that can be consumed is yellowfin tuna (*Thunnus albacares*). As a dominant commodity, tuna is targeted by fishing communities (Imron *et al.* 2019). Fishermen use traditional boats to catch tuna. Based on research results (Sinambela *et al.* 2025). It is known that yellowfin tuna can be caught from WPP-NRI 715 and 716. This fishing area can be reached by traditional "longboat" fishing vessels (Prasethea *et al.* 2025). The traditional longboat type "pelang" was originally made from nantu/nato (*Palaquium* spp./ *Payena* spp.), gopasa (*Vitex cofassus*), and limeca (*Tilia*) wood planks as the main material for fishing vessels. The characteristics of the pelang longboat are that the bow is pointed, the stern is flat with dimensions LoA = 7–9 m; B = 0.25–0.8 m; H = 0.5–1 m; T = 0.03–0.4 m, has a space in the middle, a sharp V-shaped bottom, and has an outrigger on the side of the boat which is a characteristic of the traditional pelang longboat. This pelang longboat uses a gasoline engine or outboard motor as the main propulsion system (Jassina *et al.* 2025). Additional outrigger components can be used as a balancer when the boat is operating. The outrigger's ability is to act as a balancer and maintain stability when the pelang longboat operates during fishing (Waworoentoe *et al.* 2022).

On the operational side of the sail, the use of outriggers imposes limitations by restricting the boat's maneuverability and increasing the resistance. Furthermore, damage to wooden boats frequently occurs in areas submerged in seawater. Observation results from research on wooden fishing boats (Sunardi *et al.* 2019) include fouling on the hull, weathering of the hull, broken hull boards, and holes and scratches on the hull. The phenomenon that occurs can cause a decrease in efficiency in fishing operations.

Based on observations, the current type of pelang longboat has been modified by completely changing the materials and shape of the traditional boat into a fiberglass longboat. The modifications made include making the boat from layers of fiber-reinforced plastic (FRP) arranged in layers and adding reinforcement from pipe or wood at the bottom and on the right and left sides (Rodian *et al.* 2025). The characteristics of FRP longboats are that the bow is pointed, the stern is flat with dimensions of LoA = 10–12 m; B = 0.90–1.6 m; H = 0.7–0.8 m; T empty = 0.05–0.4 m, has space in the middle, a sharp V-shaped bottom, and does not have outriggers which are the characteristics of traditional longboat body fishing vessel.

FRP technology has advantages in low cost, readily available materials and tools, and a simple fabrication process (Saputra *et al.* 2024). Several previous research topics have examined FRP boats: the advantages of traditional FRP boats (Pambudi *et al.* 2021), types of FRP materials (Boesono *et al.* 2018), and the economic comparison of traditional wooden and FRP boats (Ariesta *et al.* 2018). Previous research has focused on economic analysis and the utilization of traditional longboats. While technical aspects of seaworthiness are also important to consider in fishing operations, this topic has not been discussed in detail. The longboats currently in use are utilized for tuna fishing—powered by outboard motors and employing handline fishing gear, and carry other equipment and supplies for sea operations, including: food supplies, fuel reserves, fishing bait, ice cubes, safety equipment, and various other supporting components. Observations indicate that all specified cargo must be loaded onto the fishing vessel. However, fishermen generally do not calculate the total cargo weight and tend not to position the load in accordance with the fishing vessel's load distribution.

Frequently practiced habits can affect boat performance when operating at sea. The tendency to neglect calculating total weight and cargo placement is consistent with research (Ajamiah and Issa 2024), which states that the total cargo amount will impact speed and motion. In addition to calculating total cargo weight and load distribution, hydrostatics, resistance, engine power, and fuel consumption must be considered when determining the seaworthiness of a fishing vessel for operation (Ramadhani *et al.* 2024).

Based on the phenomenon in tuna fishing operations using traditional longboats, an evaluation of the boat design is needed, including determining hydrostatic values, simulating boat resistance, and determining fishing operation strategies. This research aims to evaluate the technical seaworthiness of longboats in planning fishing operations based on the results of vessel models according to the original shape. The evaluation process includes observation, making a boat model, operating simulations at speeds of 4, 8, 12, and 16 knots, and calculating load and fuel.

The longboat's body modeling process is obtained using Maxsurf Modeller to obtain hydrostatic values. Operational simulation to determine resistance is obtained from longboat body modeling, which is simulated at varying speeds. The research results obtained can be initial recommendations as a reference in determining fishing voyage planning.

METHODS

Materials

The research object was a traditional longboat body fishing boat with direct measurements of the main dimensions and speed of the longboat body. The sample object was a fishing boat owned by CV. Gudang Biru, a partner in the research. Seaworthiness planning research on longboat body was carried out with four strategies to obtain effective and efficient seaworthiness: (1) observation of the main dimensions to determine the parameter values of the longboat body, (2) modeling the longboat body; to determine hydrostatic values, (3) simulation of longboat body operations; to analyze resistance on the longboat body using the Wyman method, and (4) load and fuel oil calculations, to determine the seaworthiness of the longboat body.

Observation of main dimensions

Observation of research objects on traditional longboat body fishing boats was carried out in several observation stages, including: (a) identifying the type of longboat body, (b) measuring the main parameters of the longboat body, including LoA (Length Over All), LwL (Length of Water Line), BoA (Breadth Over All), H (Depth), and T (Draft), (c) conducting a review of several types of boats.

Model and simulation of the longboat body

The use of Maxsurf Modeller software in designing marine vehicles was also researched by Budiman *et al.* (2022). With an orientation to the shape of the ship's hull, the Maxsurf Modeller software can analyze the hydrostatic value and resistance of the boat when operating. Modeling of the traditional longboat body design was carried out using a direct measurement method on the research object until the longboat body design was made using the Maxsurf Modeller developed by Bentley through the following stages: (a) determining the main dimensions of the boat, (b) designing the boat model, and (c) determining the hydrostatic value of the boat (Bentley Systems 2022).

Traditional longboat body boats operating in fishing areas will be exposed to sea waves, which act as resistance on the hull. Resistance estimation is simulated on Maxsurf Resistance, developed by Bentley, through the following stages: (a) determining the ship design, (b) identifying resistance parameters, (c) testing at speed variations of 4, 8, 12, and 16 knots, based on the service speeds frequently used by the research object, and (d) analyzing the resistance values and engine power simulated using the Wyman method (Bentley Systems 2022).

Calculation of load and fuel oil

In determining seaworthiness during fishing operations, it is necessary to calculate the amount of cargo that can be loaded. Excessive components will reduce sailing range and sailing time. Furthermore, safety is determined by the longboat body capacity to accommodate all components. Exceeding the load limit can cause the longboat body to capsize and sink during operation. The load calculation stages are carried out directly: (a) determining the displacement value, (b) calculating the total load, and (c) evaluating the capabilities of the longboat body. Some of the technical information obtained can then be used to calculate the amount of fuel that can be obtained through the equation (Krivoshapov *et al.* 2020):

$$F_h = F_i \times N_i$$

The equation can be used to determine the fuel required (liters/hour) from F_i = indicative fuel use (kg/HP.hour), and N_i = power indicator (HP). Value F_i can be obtained by the equation:

$$F_i = \frac{318.4 \times \eta_{ch} \times P_0}{P_i \times \alpha \times L_0 \times T_0}$$

$$\eta_{ch} = \frac{\sum \times P_a \times T_0}{(\sum - 1) \times P_0 \times (T_a + \Delta tw + \gamma r) \times T_r}$$

$$P_i = Q \times P_{it}$$

Where the value provisions η_{ch} = filling efficiency, P_i = average indicator pressure, α = excess air coefficient, L_0 = theoretical air demand, T_0 = outside air temperature, $\sum$ = compression ratio, P_a = air pressure at the end of the suction stroke, Δtw = change in air temperature, γr = pressure of used gas, T_r = exhaust gas temperature, P_{it} = theoretical average indicator pressure, Q = correction factor, Meanwhile value N_i can be obtained by the equation:

$$N_i = \frac{P_i \times V_L \times n \times z}{60 \times 75 \times 100}$$

$$V_L = \frac{\pi}{4} \times D^2 \times L$$

$$N_e = \eta_m \times N_i$$

Where the value V_L = stroke volume, n = engine speed, z = number of cylinders, D = cylinder diameter, L = stroke length, N_e = effective power, η_m = mechanical efficiency.

RESULTS AND DISCUSSION

Characteristics of the longboat body model

A longboat is a type of boat used to search for and catch tuna. A longboat is a traditional fishing boat powered by an outboard motor. The outboard motor propulsion system consists of an engine (powerhead) as the power source, a transmission (midsection) to transmit the power, and a lower unit (water jet) that converts rotation into thrust (Supriyono *et al.* 2025). The results of the observation of the longboat, the object research are shown in Figure 1. Table 1 shows the main dimensions of the boat.

Based on observations, the characteristics of a longboat body are a pointed bow, a transom stern, a sharp V-shaped bottom, and no outriggers. The frame on a longboat body is the result of a modification of boat-manufacturing technology known as FRP technology. FRP technology has developed and become a method that is often applied by the skilled hands of craftsmen.

The longboat body is made with fiber-reinforced plastic (FRP) technology. FRP technology is a modification of conventional boat-making by making boats from wooden patterns. The basic difference from the Pelang longboat lies in the materials that make up the boat (Kamil and Purnomo 2024). Longboat bodies have advantages in terms of anti-corrosion, lightweight, easy application, and longer lifetime with FRP technology. This is in accordance with findings that FRP technology has been applied to various types of marine vehicles (Romadhoni *et al.* 2023). The bond that occurs between the filler and the matrix in the body can provide strength so that the longboat body is not easily penetrated by seawater.

Visualization of the longboat body

Figure 2 shows a visualization of a traditional longboat that was made using Maxsurf Modeller software. The modeling process was carried out by first determining the main dimensions of the traditional longboat. Next, line plans were created that refer to the original shape and size. Table 2 shows the main dimensions of the designed boat by Maxsurf. There are four model visualizations produced by Maxsurf Modeller software: (a) profile, (b) body plan, (c) plan, and (d) perspective. Figure 3a shows the main lines, namely the design water line (DWL) and water line (WL).

Figure 1. General view of the traditional longboat used for tuna fishing.

Table 1. Main dimensions of the traditional longboat used for tuna fishing.

Main Dimensions	Values (m)
LoA	10–11
BoA	0.9–1.6
H	0.6–0.8
T	0.05–0.4

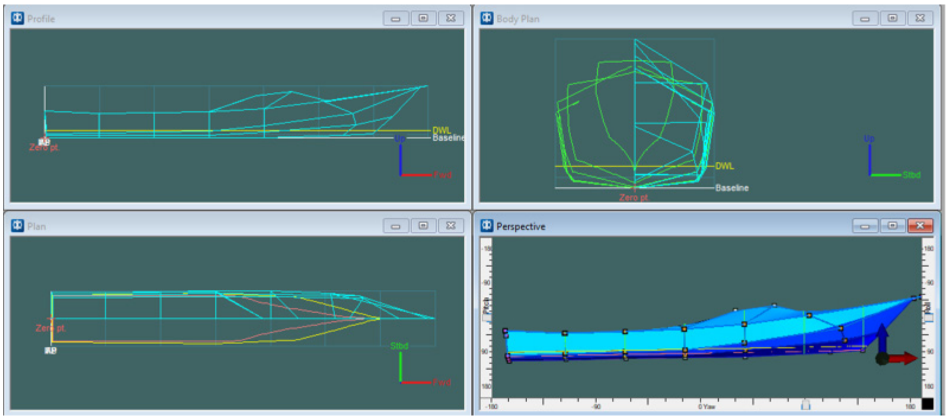

Figure 2. Three-dimensional longboat hull model generated using Maxsurf Modeller software.

Table 2. Principal dimensions of the longboat model generated using Maxsurf Modeller.

Dimensions	Value (m)
LoA	10.25
LwL	8.97
BoA	1.29
H	0.68
T	0.2

The designed waterline (DWL) value is a reference for the draft height on traditional longboats, namely 0.2 m. Meanwhile, the waterline (WL) is the value of the water draft height in the simulation, which is determined from the water level reached when the boat is operated.

Figure 3a and Figure 3b show the waterline of the longboat body on the side and front views. The existence of WL indicates the maximum immersion limit that can be calculated while the vessel operates. Figure 3c shows the boat model in its entirety, illustrating its shape and size. Based on this picture, it can be explained that the longboat body can be used for fishing by paying attention to the maximum water limit.

The hydrostatic values experienced by the longboat body can be seen in Table 3, including displacement, volume (displaced), amidships draft, submerged depth, and wetted area. The hydrostatic values for each aspect are a displacement of 1.34 tons with a displaced volume of 1.31 m³ at an operating draft of 0.20 m. The LWL value reaches 8.979 m with a maximum width at the BWL waterline of 1.297 m, resulting in an LWL/BWL ratio of ≈ 6.92. The ratio comparison results indicate that the hull characteristics of the longboat body are relatively slender. This hull shape tends to provide lower wave resistance and good propulsion efficiency at operating speeds.

Other aspects include a waterplane area of 9.454 m² and a wetted surface area of 10.904 m². Both values indicate that the majority of the longboat body area is near the water's surface. This is consistent with the characteristics of small fishing boats operating in shallow coastal waters. The TPC value of 0.097 tons/cm indicates that every additional load of around 97 kg will increase the draft of the longboat body by 1 cm, so it can be said that this type of boat is quite sensitive to changes in load.

In terms of hull shape, Cp = 0.713, Cb = 0.563, Cm = 0.792, and Cwp = 0.812 indicate a moderate hull fullness. A Cb value in the range of 0.55–0.60 indicates a reasonably good load capacity without significantly compromising hydrodynamic efficiency. BM = 0.861 m and BML = 36.034 m indicate that the metacenter is high enough relative to the center of buoyancy, thus providing good initial stability. These characteristics are suitable for fishing operations that require stability during the catching and transfer process.

The coefficient values obtained based on hydrostatic calculations in Maxsurf align with the results of research by Santoso *et al.* (2020), which compared several categories of handline fishing vessels in Kendari based on the comparison of Cp, Cb, Cm, and Cwp values. The shape and characteristics of the hull can be determined by examining the Cb value. Small and medium-sized vessels exhibit lower

Cb values; this is because the bow and stern sections of the hull undergo extreme changes in form. According to Rusmilyansari *et al.* (2017), research results indicate that the closer the block coefficient (Cb) value is to 1, the heavier the boat and the slower its maneuverability. The Cb value of 0.563 obtained for the longboat places its hull form in the intermediate range. A boat with a Cb value of around 0.5 possesses a hull shape that represents a transition between a slender vessel (chine type) and a full-bodied vessel (rounded type). Marine vessels with a high block coefficient (Cb) exhibit greater stability. This is because a larger submerged hull area results in a greater buoyant force acting on the vessel (Romadhoni *et al.* 2023)

The hydrostatic values experienced by the longboat body can be seen in Table 3. The hydrostatic displacement value is a value that needs to be considered first. This is used as initial information to determine the capabilities of the longboat body before operating. The displacement value of a boat shows the sinking weight, which means the value of the weight of liquid that can be moved by the hull of the boat (Ramadhani *et al.* 2024).

Operation of the longboat body

The waveforms that occur when the boat is operating are shown in Figure 4, which shows that a longboat body operating in the sea at a certain speed will form different waterline waves at the front, side, and rear of the boat. This figure also shows that the wake and wave patterns were formed by the movement of a longboat's hull on the water surface. When the longboat hull moves forward at a certain speed, the water around the hull changes from a calm state to a flowing state. This causes the formation of a turbulent area behind the vessel, called the wake. The wake area is a key component of viscous resistance, which influences a vessel's propulsion requirements (Molland *et al.* 2017).

The characteristics of the wake and wave patterns are crucial in hull design. A slimmer hull shape generally produces smaller waves, thereby reducing the vessel's total drag. Furthermore, the distribution of flow velocity in the wake area also affects propeller performance due to the flow conditions entering the propeller. Therefore, evaluation of wake and wave patterns is used to optimize propulsion efficiency, fuel consumption, and overall vessel performance (Molland *et al.* 2017).

The simulation results of longboat body operations at Maxsurf Resistance at various speeds are shown in Figure 5. In this simulation, the boat was operated at speeds of 4, 8, 12, and 16 knots. Simulated speed variations are adjusted from the minimum speed to the maximum speed.

Longboat hulls used for fishing operations require resistance analysis using Maxsurf Resistance software. Maxsurf Resistance is used to estimate resistance components and hydrodynamic coefficients of the hull. The parameters used in the resistance simulation process are selected to suit the characteristics of a longboat body, which is included in the category of fast boats with a slender hull shape, as shown in Table 4. Slender hull shapes are generally characterized by a large L/B ratio value, thereby reducing wave resistance and pressure drag, which has an impact on increasing hydrodynamic efficiency and ship speed performance. According to Boucher *et al.* (2018), the characteristics of slender hulls are more favorable in terms of wave drag and pressure drag, while more bulky hulls tend to have greater resistance but have higher initial stability. Thus, the LWL/BWL ratio = 6.92 can be categorized as a slender hull suitable for vessels that prioritize motion efficiency during operation, providing lower wave resistance and good propulsion efficiency at operating speeds. This is due to differences in the methods used, so the results obtained will differ based on the formulation applied (Poundra *et al.* 2017). The total resistance value of Fn (Froude number) reduction depends on the wave resistance value and Re (Reynolds number), which depends on the viscous resistance component (Tuan *et al.* 2021).

Based on the seawater wave profile in Figure 5, it can be explained that seawater waves get bigger when the speed increases. This has an impact on changes in the resistance value and power required by the boat. Operational simulation results show an increase in resistance values and power requirements in horsepower (HP): 4 knots (362.4 N and 1.25 HP), 8 knots (1449.79 N and 10.02 HP), 12 knots (2899.24 N and 30.02 HP), and 16 knots (3528.56 N and 48.68 HP). The high movement of water waves around the boat will cause an increase in the amount of frictional resistance produced by the waves (Praharsi *et al.* 2019). As a result, boats require a lot of power. On the longboat body, 2 types of outboard engines are used with a total capacity of 30 HP. The differences in HP values in the simulation can be caused by differences in the speed of the blowing sea breeze.

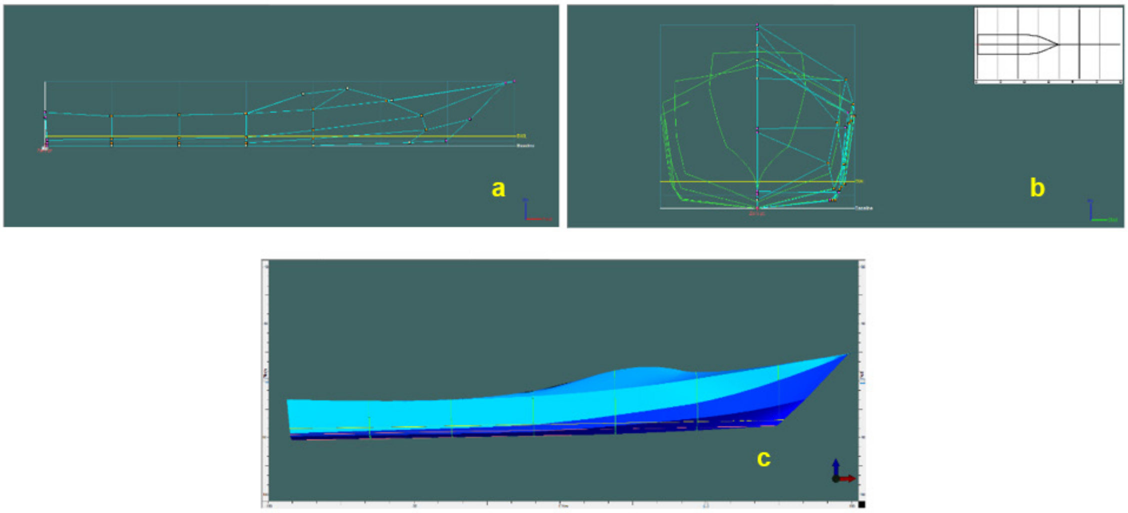

Figure 3. Views of the longboat hull model: (a) profile, (b) body plan, and (c) plan.

Table 3. Hydrostatic parameters of the longboat hull obtained from Maxsurf analysis.

No	Parameters	Values
1	Displacement	1.34 ton
2	Volume (displaced)	1.31 m^3
3	Draft amidships	0.2 m
4	Immersed depth	0.2 m
5	WL length	8.97 m
6	Beam max on WL	1.297 m
7	Wetted area	10.904 m^2
8	Max section area	0.205 m^2
9	Waterplane area	9.454 m^2
10	Prismatic coefficient (Cp)	0.713
11	Block coefficient (Cb)	0.563
12	Maximum section area coefficient (Cm)	0.792
13	Waterplane area coefficient (Cwp)	0.812
14	LCB length	3.423
15	LCF length	3.845
16	BM_t	0.861 m
17	BM_L	36.034
18	TPC	0.097 tons/cm
19	DWL	0.2 m
20	WL draft	0.1 m

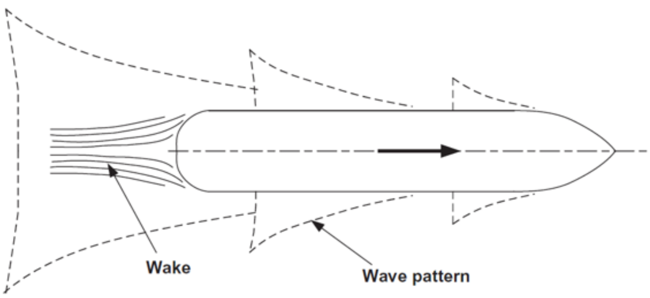

Figure 4. Wake and wave patterns around the longboat hull during operation (Molland *et al.* 2017).

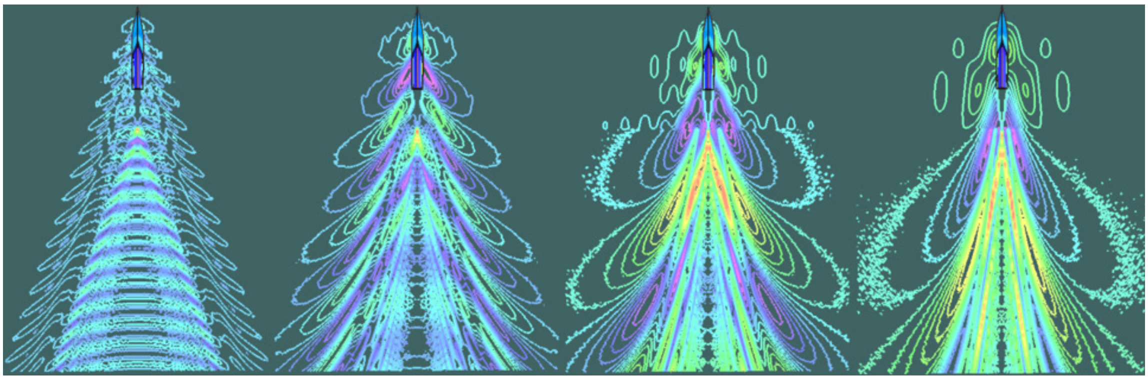

Figure 5. Wave patterns at different longboat hull speeds: (a) 4 kn, (b) 8 kn, (c) 12 kn, and (d) 16 kn.

Table 4. Parameters used in resistance simulation.

Parameters	Values
Method	Wyman
Speed	4 kn, 8 kn, 12 kn, 16 kn
Efficiency	80%
Froude Number	0.219 (4 kn), 0.439 (8 kn), 0.658 (12 kn), 0.877 (16 kn)

The simulation test results obtained indicate an increase in total resistance and power requirements as the longboat's operating speed increases. This phenomenon aligns with the research results of Bilec *et al.* (2020), which explain that fishing vessels have significantly increased ship resistance due to increased operating speed. At higher speeds, the wave-making resistance aspect becomes dominant when compared to frictional resistance, so the required propulsion engine power increases. Furthermore, another study from Setiawan *et al.* (2025) on fishing vessels in Karangantu Port tested speed variations of 5–12 knots. The simulation results showed that total resistance increased significantly with increasing operating speed, mainly due to the dominance of resistance due to wave formation that occurs at speeds exceeding 8 knots. The simulation results obtained are in accordance with theory as well as the results of experimental and numerical research on this type of fishing vessel.

The change in the longboat body speed during operation against resistance is shown in Figure 6. The resulting graph of speed variations shows a similar trend, namely an increase in resistance value along with increasing speed and Froude number. The longboat body moves slowly as the speed increases and reaches a maximum speed according to the test parameters.

At a speed of 4 knots, the resistance value is still relatively low. This is because the longboat body operates at Fn = 0.219, which is still in the frictional resistance dominance area. At this speed condition, the waves generated by the movement of the longboat body speed in the hull area are still relatively small, according to Figure 5a. Most of the power generated by the outboard motor is used to overcome friction between the hull surface and the water. This phenomenon can be seen from the shape of the curve, which is still gentle on the graph. The ratio value (LWL/BWL ≈ 6.92), indicates that the fluid flow around the hull still follows the contour and is relatively stable because the wave formation is not yet significant. According to Molland *et al.* (2017), in the range of Fn values < 0.25, the viscous resistance component still dominates the total ship resistance.

An increase in speed of 8 knots indicates that the longboat body begins to be subjected to wave resistance as one aspect of the total resistance. In this condition, the height of the bow and stern waves begins to increase due to the Froude number value, Fn = 0.439. Therefore, the increase in resistance from 362.4 N to approximately 1449.79 N is not only due to increased speed but also to the increased amount of energy lost to wave formation around the hull.

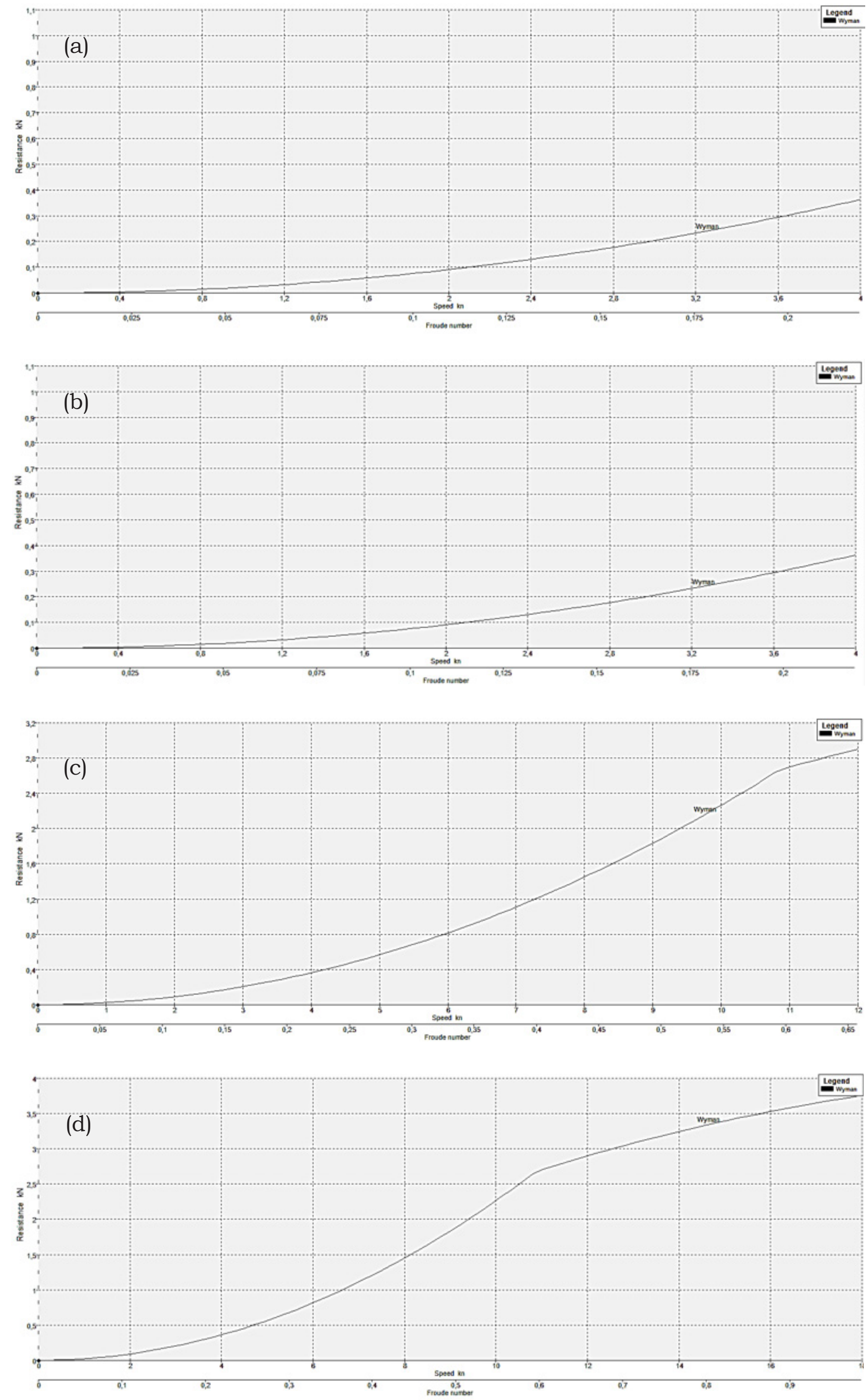

Figure 6. Resistance profile at different operating speeds: (a) 4 kn, (b) 8 kn, (c) 12 kn, and (d) 16 kn.

At a speed of 12 knots, the resulting resistance increases to approximately 2899.24 N at Fn = 0.658. This significant increase indicates that the resulting sea waves have approached the LWL value. Physically, this phenomenon is often referred to as the hull speed region, meaning the longboat is in a state midway between the bow and stern waves. This phenomenon aligns with research by Naryanto *et al.* (2024), which explains that the wave resistance component on traditional fishing vessels increases sharply in the Fn range of 0.35–0.60. An increase in speed to 16 knots indicates an increase in resistance of 3528.56 N at Fn = 0.877. This may indicate that the streamlined hull shape can produce more efficient flow distribution, resulting in less pronounced wave resistance. The change in wave patterns and pressure distribution around the hull causes the resistance rate to begin to approach a stable condition.

Calculation of cargo and fuel oil

The longboat body needs to pay attention to cargo and safety aspects to determine voyage planning. The cargo aspect can be seen from the total amount of cargo that can be loaded on the boat. Some components and equipment on the boat are shown in Table 5.

The main components needed during operations at sea include food supplies, fuel reserves, fishing bait, and ice cubes. Table 5 shows the total weight of the boat, which is 1,290 kg or 1.29 tons, which is still below the displacement limit of 1.34 tons. This indicates that the longboat load capacity is operating within its load capacity. When departing for the fishing grounds, the total final load can be planned and calculated to ensure the load does not exceed the carrying capacity. Upon returning to the fishing base after fishing operations, the longboat will experience an uncertain load due to excess fish and the reduction of ice weight from melting. The total load value is not a fixed figure, as the number of tuna caught may vary depending on the catch at the fishing grounds. Furthermore, the amount of ice loaded can also melt, reducing the total weight (Iqbal *et al.* 2023).

The difference between the total weight and the load can be used as a guideline for determining the amount of free space to load or not, and can be used as a safety and security factor to consider. Safety aspects that need to be considered are based on the total weight and distribution of the load on the longboat body. Reducing the total payload can increase operational efficiency and effectiveness due to the lighter load on the longboat. The level of catch fluctuation is consistent with research (Wahyudin *et al.* 2022), which states that the number of fish caught depends on conditions and weather in the fishing area.

In addition to the main and supporting components of fishing operations, fishermen are required to plan for fuel requirements during operation. The longboat body used in this study uses a Yamaha E15DMH outboard engine. The main specifications of this outboard engine are shown in Table 6.

Table 5. Components carried on board the longboat.

Objects	Weights (kg)	Quantities	Values (kg)
Fish and ice	450	2	900
Main fuel tank	24	2	48
Reserve fuel tank	35	1	35
Fisherman	50	2	100
Food and materials	40	1	40
Plywood	4	3	12
Outboard engine, 15 HP	30	2	60
Boat	95	1	95
		Total	**1,290 kg**

Table 6. Specifications of the Yamaha E15DMH outboard engine.

Parameter	Value
Engine	Yamaha E15DMH (15 PK)
Cylinder	246 cc
Bore × stroke	56 mm × 50 mm
Engine speed	4,500–5,500 rpm
Compression ratio	7

Based on the results of modeling and simulation, as well as outboard engine specification data, estimates of engine power and service speed during operation can be obtained. Based on all equations in the method, an estimate of the amount of fuel needed based on engine specifications can be obtained if operated at varying speeds of 4 knots (0.51 liters/hour), 8 knots (4.14 liters/hour), 12 knots (12.12 liters/hour), and 16 knots (19.58 liters/hour). The amount of fuel required has increased; this is due to effective power factors, mechanical efficiency, and the use of indicator fuel (Tumigolung *et al.* 2017). The need for proper calculations before fishing is the main key to effective, efficient, and safe fishing operations (Wijianto *et al.* 2025).

CONCLUSION

Traditional longboat body boats can be used as one of the vehicles in fishing operations. When carrying out fishing operations, it is necessary to conduct a technical evaluation of the fishing operation planning, including modeling and simulation of longboat bodies at certain speeds, load calculations, fuel calculations, and safety aspects. Evaluation of technical seaworthiness based on observations and modeling results indicates that the "longboat body" is a type of traditional boat with an LWL/BWL ratio of 6.92, classified as a slender hull. The hull shape has a tendency to provide lower wave resistance and good propulsion efficiency at operating speeds. Simulation of resistance at speed variations shows that the higher the operating speed, the greater the waves generated at the bow and stern, which impacts the high resistance of the boat hull at 4 knots (362.4 N and 1.25 HP), 8 knots (1449.79 N and 10.02 HP), 12 knots (2899.24 N and 30.02 HP), and 16 knots (3528.56 N and 48.68 HP). The total load that the longboat body can accept is 1.29 tons, with a maximum limit of 1.34 tons. The difference between the load and displacement is one of the safety aspects. According to voyage planning, the longboat body is operated by 2 outboard engines with estimated fuel requirements at 4 knots (0.51 liters/hour), 8 knots (4.14 liters/hour), 12 knots (12.12 liters/hour), and 16 knots (19.58 liters/hour). The technical seaworthiness aspects that have been established can serve as a reference for planning effective, efficient, and safe fishing voyages.

ACKNOWLEDGEMENT

The authors would like to thank the Department of Mechanical Engineering, Universitas Muhammadiyah Surakarta, the Department of Fisheries Mechanization, and the Department of Fisheries Technology at Politeknik KP Bitung and CV. Gudang Biru for the support and funding provided to this researcher so that the research could be completed on time.

REFERENCES

Ajamiah AA, Issa H. 2024. Study the Stability of a High-Speed Boat According to the Recommendations of Maritime Classification Societies. *International Research Journal of Engineering and Technology*. 11(10): 347–354.

Ariesta RC, Arif MS, Puspitasari HP. 2018. Comparison of Economical Analysis of Wood and Fiberglass Vessels in Randuboto Village, Gresik Regency, East Java. *ECSOFiM: Economic and Social of Fisheries and Marine Journal*. 6(1): 73–82. DOI: https://doi.org/10.21776/ub.ecsofim.2018.006.01.07.

Bentley Systems. 2022. *Naval Architecture Applications for All Types of Vessels*. Exton (US): Bentley Systems

Bilec M, Obreja CD. 2020. Ship Resistance and Powering Prediction of a Fishing Vessel. *ModTech International Conference - Modern Technologies in Industrial Engineering VIII, June 23–27, 2020, Iasi, Romania*. IOP Conference Series: Materials Science and Engineering. DOI: https://doi.org/10.1088/1757-899X/916/1/012011.

Boesono H, Saraswati M, Setiyanto I. 2018. Analisis Penggunaan *Foam Polyurethane* pada Kapal Ikan 5 GT sebagai Daya Apung Cadangan di PT. Jelajah Samudera Internasional Kabupaten Jepara. *Saintek Perikanan: Indonesian Journal of Fisheries Science and Technology*. 13(2): 82–88. DOI: https://doi.org/10.14710/ijfst.13.2.82-88.

Boucher JP, Labbe R, Clanet C, Benzaquen M. 2018. Thin or Bulky: Optimal Aspect Ratios for Ship Hulls. *Physical Review Fluids*. 3(6): 1–9. DOI: https://doi.org/10.1103/PhysRevFluids.3.074802.

Budiman Y, Romansyah F, Rochim MN,

Akmal MS, Solikin M, Yudianto A. 2022. Perancangan Bodi Kapal Patroli Lepas Pantai : Analisis Numerik Hidrodinamika Bodi Deep V-Hull, Bulbous Hull, dan Catamaran Melalui Simulasi Software Maxsurf. *Prosiding Seminar Nasional Ilmu Teknik dan Aplikasi Industri Fakultas Teknik Universitas Lampung*. 5: 122–127.

Iqbal M, Terziev M, Tezdogan T, Incecik A. 2023. Operability Analysis of Traditional Small Fishing Boats in Indonesia with Different Loading Conditions. *Ships and Offshore Structures*. 18(7): 1060–1079. DOI: https://doi.org/10.1080/17445302.2022.2107300.

Imron M, Yusfiandayani R, Baskoro MS. 2019. Produksi dan Produktivitas Tuna oleh Kapal Tuna *Longline* yang Berbasis di PPN Palabuhanratu. *Jurnal Teknologi Perikanan dan Kelautan*. 10(2): 173–181. DOI: https://doi.org/10.24319/jtpk.10.173-181.

Jassina SN, Fadillah A, Nikmatulliah MI. 2025. The Design of Hydrofoil Boat for Supporting Water Tourism and Transportation in Lake Toba. *The 5th EPI International Conference on Science and Engineering (EICSE) 2021, September 28–29, 2021, Gowa, Indonesia*. AIP Conference Proceedings. DOI: https://doi.org/10.1063/5.0270277.

Kamil F, Purnomo J. 2024. Evaluation of Compressive Strenght of Concrete with Replacement of Conventional Coarse and Fine Aggregates Using Palm Kernel Shell and Coconut Husk. *Dinamika Teknik Sipil: Majalah Teknik Sipil*. 17(2): 60–67. DOI: https://doi.org/10.23917/dts.v17i2.6167.

Krivoshapov SI, Nazarov AI, Mysiura MI, Marmut IA, Zuyev VA, Bezridnyi VV, Pavlenko VN. 2020. Calculation Methods for Determining of Fuel Consumption per Hour by Transport Vehicles. *26th Technical and Scientific Conference "Transport, Ecology – Sustainable Development" Eko Varna 2020, October 8–10, 2020, Varna, Bulgaria*. IOP Conference Series: Materials Science and Engineering. DOI: https://doi.org/10.1088/1757-899X/977/1/012004.

Molland AF, Turnock SR, Hudson DA. 2017. *Ship Resistance and Propulsion: Practical Estimation of Ship Propulsive Power* (*Second Edition*). Cambridge (GB): Cambridge University Press.

Naryanto RF, Bahatmaka A, Wibowo MY, Izzuddin MH, Buana LP, Pratama RD, Fahmi FF, Ghyferi AA. 2024. Analyzing The Total Resistance and Wave Pattern of Modification Hull Form Design Catamaran Fishing Vessel. *Wave: Jurnal Ilmiah Teknologi Maritim*. 18(2): 99–106. DOI: https://doi.org/10.55981/wave.2024.2165.

Pambudi S, Asrofi M, Triono A, Tsabit MZB, Murtadho NA. 2021. Perahu *Fiberglass* untuk Penunjang Alat Penangkap Ikan dan Sektor Pariwisata Desa Sumberasri Kecamatan Purwoharjo Banyuwangi. *Jurnal Pengabdian Masyarakat Berkemajuan*. 4(3): 723–727. DOI: https://doi.org/10.31764/jpmb.v4i3.4843.

Poundra GAP, Utama IKAP, Hardianto D, Suwasono B. 2017. Optimizing Trimaran Yacht Hull Configuration Based on Resistance and Seakeeping Criteria. *Procedia Engineering*. 194(1): 112–119. DOI: https://doi.org/10.1016/j.proeng.2017.08.124.

Praharsi Y, Jami'in MA, Suhardjito G, Wee HM. 2019. The Comparison of Characteristics Profile of the Traditional Fishing Boats in Lamongan, Probolinggo, and Pasuruan, Indonesia. *Proceedings of the International Conference on Industrial Engineering and Operations Management, July 23-26, 2019, Pilsen, Czech Republic*. IEOM Society International. DOI: https://doi.org/10.46254/EU03.20190316.

Prasethea KF, Suyanto S, Sundari MS. 2025. Determinants of Technical Efficiency in Indonesian Manufacturing: The Case of Motor-Vehicle Firms. *Jurnal Ekonomi Pembangunan: Kajian Masalah Ekonomi dan Pembangunan*. 21(2): 81–90. DOI: https://doi.org/10.23917/jep.v21i2.10634.

Ramadhani AI, Tjahjana DDDP, Purwanto A, Nizam M. 2024. Feasibility of Electric Fishing Boats Based on Evaluation of Hydrostatic Forces and Resistance. *Journal of Advanced Research in Fluid Mechanics and Thermal Sciences*. 116(2): 75–87. DOI: https://doi.org/10.37934/arfmts.116.2.7587.

Rodian A, Paundra F, Afisna LP, Nurullah FP, Pujiyulianto E. 2025. The Effect of Variations in PVC Foam Core Thickness on the Failure Analysis of Bending Test in Sandwich Composite. *Media Mesin: Majalah Teknik Mesin*. 26(1): 16–25. DOI: https://doi.org/10.23917/mesin.v26i1.6108.

Romadhoni, Santoso B, Purwoko S, Nasution P. 2023. Analisa Desain dan Kalkulasi Biaya Pembangunan Kapal Perikanan 5 GT Berbahan *Fiberglass* untuk Perairan Riau. *Journal of Management and Business.* 5(2): 964–976. DOI: https://doi.org/10.31539/jomb.v5i2.5874.

Rusmilyansari R, Rosadi E, Iriansyah I. 2017. Technical Suitability and Static Stability of Sungkur Fishing Boats for Fish and Shrimp Catching. *The 2nd International Conference on Applied Marine Science and Fisheries Technology (MSFT), August 22–25, 2017, Langgur City, Southeast Maluku, Indonesia.* IOP Conference Series: Earth and Environmental Science. DOI: https://doi.org/10.1088/1755-1315/89/1/012007.

Santoso AW, Novita Y, Iskandar BH, Baskoro MS. 2020. Fishing Boat Design Based Local Wisdom in Southeast Sulawesi Fishermen. *American Journal of Software Engineering and Applications.* 9(1): 1–18. DOI: https://doi.org/10.11648/j.ajsea.20200901.11.

Saputra H, Cahyagi D, Perkasa VN, Purnama D, Nurmannsyah O, Saputra R, Ferari R, Fauzy FIA, Fadillah M. 2024. Design and Fabrication of 6 Meter Fiberglass Boat for Coastal Water Tourism in Batam. *International Journal of Marine Engineering Innovation and Research.* 9(2): 370–377. DOI: https://doi.org/10.12962/j25481479.v9i2.20342.

Setiawan NA, Satria D, Pinem MP, Suprayogi DT. 2025. Analysis of Resistance on Fishing Vessels on Fisheries Port, Karangantu Serang. *Timer: Trends in Mechanical Engineering Research.* 3(1): 21–26.

Sinambela CB, Pratasik SB, Makapedua DM, Sumilat DA, Luasunaung A, Budiman J, Andaki JA, Natalia DA. 2025. Yellowfin Tuna Catch Demographics by Size and Sex Ratio at Bitung Ocean Fishing Port. *Jurnal Pesisir dan Laut Tropis.* 13(2): 95–102. DOI: https://doi.org/10.35800/jplt.13.2.2025.61486.

Sunardi, Sukandar, Sulkhani EY, Rahman MA. 2019. Repair Technique for Wooden Fishing Boats Using Fibreglass. *The 2nd International Symposium on Marine Science and Fisheries (ISMF2), June 22, 2019, Makassar, Indonesia.* IOP Conference Series: Earth and Environmental Science. DOI: https://doi.org/10.1088/1755-1315/370/1/012081.

Supriyono H, Supardi A, Romadhon MRN, Yulianto A, Utomo UB. 2025. Designing Electric Braking System for Brushless Direct Current Motor as an Electric Bicycle Propulsion. *Bulletin of Electrical Engineering and Informatics.* 14(2): 986–995. DOI: https://doi.org/10.11591/eei.v14i2.8608.

Tuan VT, Huy PN, Phoemsapthawee S, Kreuawan S. 2021. E-Engine for a Long-Tail Boat, an Application in ASEAN (Association of Southeast Asian Nations)-Design and Comparison with Internal Combustion Engine. *World Electric Vehicle Journal.* 12(1): 1–11. DOI: https://doi.org/10.3390/wevj12010036.

Tumigolung SS, Pangalila FPT, Kaparang FE. 2017. Studi tentang Pengaruh Perbedaan Daya Mesin terhadap Kecepatan dan Konsumsi Bahan Bakar Minyak pada Perahu Pakura. *Jurnal Ilmu dan Teknologi Perikanan Tangkap.* 2(5): 187–193. DOI: https://doi.org/10.35800/jitpt.2.5.2017.15943.

Wahyudin I, Darma YYE, Prasetya IGNAS, Insprasetyobudi H. 2022. Preliminary Design of Traditional Fishing Boat (2 GT) with Additional Floating Compartment for Safety Reasons Using BKI Rules. *International Journal of Marine Engineering Innovation and Research.* 7(4): 321–334. DOI: https://doi.org/10.12962/j25481479.v7i4.13266.

Waworoentoe RSAR, Dien HV, Kalangi PNI, Kaparang FE, Modaso VOJ, Pangalila FPT. 2022. Studi Tentang Tahanan Perahu Pelang di Desa Rap-Rap Kabupaten Minahasa Selatan. *Jurnal Ilmu dan Teknologi Perikanan Tangkap.* 7(2): 117–121. DOI: https://doi.org/10.35800/jitpt.7.2.2022.41745.

Wijianto, Sarjito, Subroto, Faishal A, Supriyono, Anam K. 2025. Analysis of the Impact of Installing CAI and IMS on a Motorcycle Engine. *Journal of Applied Engineering Science.* 23(4): 656–663. DOI: https://doi.org/10.5937/jaes0-55707.